

NASA Technical Memorandum 102439

# Thermo-Oxidative Stability Studies of PMR-15 Polymer Matrix Composites Reinforced With Various Continuous Fibers

Kenneth J. Bowles  
*Lewis Research Center*  
*Cleveland, Ohio*

Prepared for the  
35th International SAMPE Symposium and Exhibition  
Anaheim, California, April 2-5, 1990



(NASA-TM-102439) THERMO-OXIDATIVE STABILITY  
STUDIES OF PMR-15 POLYMER MATRIX COMPOSITES  
REINFORCED WITH VARIOUS FIBERS (NASA) 16 p  
CSCL 110

N90-19310

Unclas  
0271807

G3/24

Trade names or manufacturers' names are used in this report for identification only. This usage does not constitute an official endorsement, either expressed or implied, by the National Aeronautics and Space Administration.

THERMO-OXIDATIVE STABILITY STUDIES OF PMR-15 POLYMER MATRIX  
COMPOSITES REINFORCED WITH VARIOUS CONTINUOUS FIBERS

Kenneth J. Bowles  
National Aeronautics and Space Administration  
Lewis Research Center  
Cleveland, Ohio 44145

SUMMARY

An experimental study was conducted to measure the thermo-oxidative stability of PMR-15 polymer matrix composites reinforced with various fibers and to observe differences in the way they degrade in air. The fibers that were studied included graphite and the thermally stable Nicalon and Nextel ceramic fibers. Weight loss rates for the different composites were assessed as a function of mechanical properties, specimen geometry, fiber sizing, and interfacial bond strength. Differences were observed in rates of weight loss, matrix cracking, geometry dependency, and fiber-sizing effects. It was shown that Celion 6000 fiber-reinforced composites do not exhibit a straight-line Arrhenius relationship at temperatures above 316 °C.

INTRODUCTION

Current interest in aircraft engine structure applications is focused on polymer matrix composites with use temperatures as high as 371 °C and eventually up to 416 °C. Depending upon the nature of the structure in which it is to be used, the composite material must maintain its structural integrity for times ranging from 100 hr to over 5000 hr in air at atmospheric and elevated pressures.

It has been observed in the past that the thermo-oxidative stability of polymer matrix composites was strongly influenced by the reinforcement (refs. 1 to 5). It has also been reported that graphite fibers containing significant amounts of sodium and potassium as contaminants were less thermo-oxidatively stable than those graphite fibers with a low alkali metal content (refs. 1 to 4).

A recent study (ref. 5) has shown that the combination of the PMR-15 polyimide matrix and the Celion 6000 graphite fiber, obtained from BASF Structural Materials Inc., appears to have a synergistic effect on the thermo-oxidative stability of composites made from these two materials. In reference 6, it is shown that this fiber-matrix interface is the location of a very aggressive reaction at high temperature, with the fiber experiencing the more severe degradation.

If the use temperature of graphite fiber-reinforced composites is to be raised, then it appears from the literature that the thermo-oxidative stability of the reinforcement will have considerable influence on successfully sustaining high-temperature performance from polymer matrix composites.

The purpose of this work was to measure the thermo-oxidative response of PMR-15 composites in air and to observe possible differences in the degradation mechanisms of composites reinforced with more thermally stable fibers.

The ultimate objective of this study was to provide a better understanding of the effect of fiber-matrix bonding efficiency on the thermo-oxidative stability of PMR-15 composites and to examine the role of the reinforcement material in influencing the rate of composite weight loss.

## MATERIALS

Three monomers were used in preparing the 1500 molecular weight PMR-15 polyimide matrix. These included the monomethylester of 5-norbornene-2,3-dicarboxylic acid (NE), 4,4'-methylenedianiline (MDA), and freshly esterified 3,3',4,4'-benzophenonetetracarboxylic dianhydride (BTDA). These materials were obtained from commercial sources.

Esterification of BTDA to the dimethyl ester of 3,3',4,4'-benzophenone tetracarboxylic acid (BTDE) was accomplished by refluxing the anhydride in methanol to form a 50 wt % BTDE solution. The monomer solution was prepared at room temperature by the addition of the monomers in a 2 NE: 3.087MDA: 2.087 BTDE stoichiometric ratio with the proper amount of methanol to make a 50 wt % solution.

The reinforcements used in this study were the Thornel T-40R graphite fiber (Amoco), the Nicalon silicon carbide fibers (Nippon Carbon Co.), and the Nextel 312 aluminum oxide-boron oxide-silicon oxide fiber (3M Corp.). The properties of these fibers are given in table I. All of the fibers were unsized except for the Nicalon and Nextel fibers. Two batches of Nicalon fibers were used. One batch was sized with polyvinyl acetate (PVA) and the second was sized with a bismaleimide compatible sizing (BMIC). Some of the PVA-sized fibers were stripped with acetone to remove the sizing. This fiber is referred to herein as stripped or unsized Nicalon. The Nextel 312 fiber was sized with a polyimide compatible (PIC) sizing designated as A1100 silane.

## LAMINATE FABRICATION AND SPECIMEN PREPARATION

The following steps were employed in prepregging and laminate fabrication:

- (1) Fiber tow winding
- (2) Tow impregnation by the monomer solution
- (3) Drying
- (4) Ply cutting and layup
- (5) Imidization
- (6) Compression molding

This procedure, fully described elsewhere (ref. 6), yielded low-void, high-quality laminates. All the laminates were examined nondestructively by the through-transmission C-scan method. A free-standing post cure in air at 316 °C for 16 hr was used to complete the curing process.

A series of five 10-ply T-40R fiber-reinforced and three 12-ply Celion 6000 reinforced unidirectional composite laminates were fabricated. The laminates had nominal dimensions of 20.3 cm in the fiber direction by 7.6 cm transverse to the fibers and were approximately 0.18 cm thick. The laminates were machined into specimens having the following approximate dimensions:

- (1) 2.5 by 7.6 cm coupons
- (2) 6.35 by 0.51 cm flexural specimens
- (3) 2.54 by 0.51 cm shear specimens

Two unidirectional twelve-ply laminates of each ceramic fiber-reinforced composite were fabricated. They measured 20.3 cm in the fiber direction by 7.6 cm in the transverse direction. The Nicalon and Nextel composite laminates measured 0.21 cm and 0.23 cm in thickness, respectively.

### TEST PROCEDURE

The thermal aging was done in air convection ovens. The change rate of the air was 100 cm<sup>3</sup>/min. The specimens were allowed to cool to room temperature in a desiccator before being weighed. Specimen dimensions were measured and recorded every time the specimens were removed from the oven for weighing. Fiber specimens were aged in large Petri dishes with stainless steel screens fitted across the open top.

The mechanical properties that were measured were flexural and shear strengths and flexural moduli. The apparent horizontal shear strength was determined by using the short-beam method as detailed in ASTM-D2433. The two support pins measured 0.64 cm in diam instead of the recommended 0.32 cm diam, and a span-to-depth ratio of 5:1 was used. The flexural properties were measured with the procedure described in ASTM-D790. A span of 6.4 cm was used. This span produced a span-to-depth ratio of 26:1 for most of the flexural specimens tested.

The void contents of the composites were measured by using an H<sub>2</sub>SO<sub>4</sub>/H<sub>2</sub>O<sub>2</sub> digestion technique (ASTM D3171) with composite density measurement data (D-792). Nextel reinforcement composite fiber volumes were determined by thermal gravimetric analyses (the burning off of the matrix).

Fiber surface areas and pore sizes were measured with a Micromeritics Digisorb 2500 BET gas adsorption-desorption analyzer. Nitrogen and krypton were the gases used to measure the surface areas.

### EXPERIMENTAL RESULTS

Weight loss measurements for bare, unsized T-40R graphite fiber are plotted in figure 1 for times up to 3200 hr. The Arrhenius constants calculated from these data are listed in table II along with those of Celion 6000 graphite fiber (ref. 6), some PMR-15 composites, and PMR-15 neat resin (ref. 6). The weight loss data from the 316 °C isothermal aging test of Celion 6000/PMR-15 composites (ref. 6) are presented in figure 2. Also shown are weight loss data for stripped Nicalon, PVA and PMIC sized Nicalon, and PIC sized Nextel 312, Celion 6000, and T-40R fiber-reinforced PMR-15 composites. The thermo-oxidative stability for neat resin PMR-15 (ref. 6) and the calculated rule-of-mixtures values for a 60-fiber vol % composite are also included in figure 2 for reference. The weight loss data are presented in the figure on the basis of weight loss per unit surface area.

Weight loss data from air-aging tests of Celion 6000/PMR-15 composites (measured in this study at temperatures below 288 °C) were used to calculate activation energies for the degradation process. The temperatures at which the tests were conducted were 204, 260, and 288 °C. The data are plotted in figure 3. The activation energies that were calculated for aging times of 3015, 3469, 3990, and 4545 hr are 23.2, 22.3, 23.6, and 29.0 Kcal/g-mol, respectively. These measurements were made to extend the data range below 300 °C.

Interlaminar shear strength (ILSS) and flexural test data are listed in table III. The data listed are averages from four specimens. Measured short-beam shear strengths and three-point flexural strengths of PMR-15 unidirectional composites reinforced with the three ceramic fibers are presented in table III. Typical strength values for Celion 6000 graphite fiber-reinforced composites are also listed for comparison (ref. 7).

The results of the BET fiber surface area measurements are given in figure 4. Results show that as the surface area of the Celion 6000 graphite fiber increases, a significant amount of fiber porosity develops and also increases. The pore concentration increases with the aging time and the pore diameters average 50 Å.

## DISCUSSION

### Mechanical Properties

The Celion 6000/PMR-15 composite material displays high flexural strength and good interlaminar shear strength. The magnitudes of these property values indicate that there is a good interfacial bond between the fiber surface and the matrix material. The efficiency of the bonding is confirmed by SEM pictures of a surface that was cleaved with a razor blade parallel to the fibers. These pictures show matrix material firmly attached to the fiber surfaces along the cleaved surface (see fig. 5). In contrast, the unsized and PVA-sized Nicalon fiber-reinforced PMR-15 composites exhibit flexural strengths of about 60 percent of the Celion 6000 fiber-reinforced composites and about one-third of the interlaminar shear strength.

SEM photographs of these composites (fig. 6) show bare fiber surfaces along the cleaved surface, indicating low bonding strength. The BMIC Nicalon fiber-reinforced composites possess better mechanical properties than the Celion 6000 fiber-reinforced composites. Figure 7 is an SEM photograph of a cleaved surface of the composite that was reinforced with the BMI compatible sizing. Note that no matrix debris is attached to the fiber surface as is shown for the Celion 6000 composites in figure 5. This photograph (fig. 7) presents no visual evidence of the effectiveness of the sizing in promoting good interfacial bonding between the fiber and the matrix. The Nextel 312 composites were made from fiber that was sized with PIC sizing. The mechanical properties are also listed in table III.

The T-40 unsized graphite fiber-reinforced composites possess mechanical properties of about the same magnitude as the ceramic fibers. The interlaminar shear strength (ILSS) and the flexural strength are less than those of the Celion 6000 graphite fiber-reinforced composites. The greatest difference in strength is seen to be in flexure. The T-40 composites have a flexural

strength almost one-half that of the Celion 6000 composites. The reason for the low values for T-40R mechanical properties may be due to surface features such as chemistry or density of active sites. Figure 8 shows a surface of the T-40R reinforced composite that was cleaved with a razor blade. Note the bare surfaces and the deep striations in the surfaces parallel to the axes. The rough surface should enhance mechanical bonding but it does not appear to do so judging from the lack of fiber surface bonding shown in figure 8 and the composite mechanical properties measured with these specimens.

In table III, the rule-of-mixtures value for the tensile strength of each type of laminate is listed underneath the measured value of the flexural strength. The tensile values are not equivalent to the flexural strengths. However, if we compare the measured values with the calculated values, all the measured values lie between 66 and 74 percent of the rule-of-mixtures values except those for the T-40R and DMIC sized Nicalon composites. The flexural strengths of composites are normally a bit higher than the composite tensile strengths. This accounts for the strength ratios being higher than the rule-of-mixtures value of 60 percent. The T-40 reinforced composite has a flexural strength 44 percent as great as the calculated tensile strength. This is puzzling since the flexural strength is a fiber-dominated property.

Equally puzzling is the behavior of the BMIC sized Nicalon composite, which has a flexural strength equal to 135 percent of its calculated tensile strength. Similar behavior is noted in reference 9. One cause may be the "healing" of the fiber surface defects and weak spots by the matrix. The interlaminar shear strength is a matrix- and interface-controlled property. It is evident that the properties for the Celion 6000 and the BMIC sized Nicalon listed in table III are exceptionally good values. The values in the same table for the other ceramic fiber-reinforced composites are very low. The value for the T-40R reinforced composite is acceptable and does not reflect the condition one would expect from a weak or nonexistent interfacial bond. Again, the high shear strength of the BMIC sized Nicalon composite is not reflected in the SEM picture in figure 7. Further study is needed to clarify these inconsistencies.

### Geometry Effect

Previous aging studies (refs. 1 to 4) identify a substantial specimen size effect on weight loss rates for graphite fiber-reinforced polymer matrix composites. For Celion 6000/PMR-15, this is shown to be due to edge effects (refs. 4 and 5) with the most rapid weight loss occurring at the edge surfaces containing graphite fiber ends. These surfaces commonly exhibit an erosive appearance with interfiber cracks running parallel to the fibers. The cracks extend a measurable distance into the body of the composite specimen (greater than 0.7 cm (ref. 6)). The additional surface area resulting from this type of degradation allows a much more aggressive attack at the specimen end surface than is observed on other types of surfaces.

Not all of the specimens aged in this study behaved in this manner. This extreme amount of surface attack and interfiber end cracking did not occur during the aging of the ceramic fiber composites or the T40-R graphite reinforced polymer matrix composites. A comparison of fiber end composite surfaces for Celion 6000 and T-40 reinforced composites is shown in figure 9. Small cracks were observed in these ends. They were oriented between the plies rather than through them.

There was no evidence of the excessive degree of size effects from weight loss rates measured with aged composites reinforced with ceramic fibers. The weight losses of each of three different sizes of specimens were about the same at corresponding times. The T-40R graphite fiber-reinforced composites did not appear to lose weight in the same way as did the Celion 6000 fiber-reinforced composites. Three different sizes of specimens were aged in this study. The sizes were as follows: (1) 7.62 by 2.54 by 0.20 cm, (2) 2.54 by 0.51 by 0.20 cm, and (3) 1.27 by 0.51 by 0.20 cm. Weight loss rates for these three sizes were about the same at 316 °C during the first 400 hr (fig. 10).

After the initial similar weight loss behavior for specimens of the three different sizes, it appeared that the weight loss rates for the T-40 reinforced composites might be correlatable with the cut surface areas that were perpendicular to the longitudinal axes of the fibers. As time elapsed, the smaller specimens started to exhibit greater weight loss rates than the larger size specimens. This relationship appeared to be common to the set of T-40R/PMR-15 composite materials that were fabricated and tested. The calculated rate of oxidation of the fiber end surfaces of the T-40R specimens was not as large as that previously determined for the Celion 6000 composites (ref. 6).

#### Thermo-Oxidative Behavior

The isothermal aging weight losses of the six different fiber-reinforced composites at 316 °C are shown in figure 2 on a weight-per-unit-area basis. The thermo-oxidative ranking of these different types of PMR-15 composites is as follows: (1) Celion 6000, (2) T-40R, (3) Nextel, (4) BMIC sized Nicalon, (5) unsized Nicalon, and (6) PVA sized Nicalon. The calculated rule-of-mixtures weight loss values, based on the neat resin data, are included in figure 2. Except for the PVA sized Nicalon reinforced fibers, the two ceramic fiber-reinforced composites showed weight loss behavior similar to the calculated rule-of-mixtures curve. In contrast, the two graphite fiber-reinforced composites exhibited repressed weight losses in relation to the same curve. This confirmed the results of previous studies reported in reference 6. The slopes of the curves for the stripped and PVA sized Nicalon composites were similar. The reason for the higher weight loss of the PVA sized composite was probably due to the sizing itself because PVA degrades at a very low temperature. The percentage difference shown in figure 2 seems to support this conclusion because the difference between the two curves is about 1 percent. The normal value for weight percent of the sizing on graphite fibers is about 1 percent.

Arrhenius activation energies for the different types of polyimide composites are listed in table II. The activation energies were calculated by two different methods. The first method involved the use of the slopes of the initial, linear portions of the weight-loss/time-curves at each temperature. In the second method, a curve-fitting procedure was used for the same individual weight loss curves to obtain the rates. There were only slight differences in the two sets of calculated energies. It appeared that the differences in weight loss rates between the different types of composites were not reflected by significant differences in these activation energies. The more stable graphite composites seemed to possess lower activation energies than the ceramic composites over the temperature range investigated.

The differences between the activation energies of the composites and the ceramic fibers, however, were such that the more stable composite (Nextel) had the highest activation energy, while the least stable (stripped Nicalon) had the lowest energy. The Celion 6000 graphite fiber had a different activation energy than the T-40R fiber, but the T-40R fiber was much more thermo-oxidatively stable than the Celion 6000 fiber. None of the composites possessed an activation energy close to that of the neat PMR-15 resin at 316 °C. It appears from this data that there may be a difference in the oxidation mechanisms of the two types of composites (ceramic and graphite). It might be inferred that the differences in the rate of weight loss between the two kinds of composites (ceramic and graphite) could be caused by weak interfacial bonding, consisting of only a mechanical bond or Van der Waals bonds. This type of bonding may allow oxygen diffusion to occur along the fiber/matrix interfaces into the interior of the Nicalon reinforced composites. This would result in internal oxidation of the specimens. The ceramic and graphite fibers had about the same CTE's in the radial direction; therefore, oxygen diffusion or penetration into the composites through interfacial separations should not be a significant factor. Access due to less intimate contact at temperatures approaching the curing temperature of 316 °C should be the same for both types of fibers under the above conditions.

No size effect was found from the aging data for the ceramic fiber-reinforced composites. However, the accelerated oxidation rate at the fiber end surfaces for the Celion 6000 reinforced composites was due to the heavy cracking and the resultant increase in surface area which somehow must be related to differences (other than interfacial bonding) in the Celion 6000 fiber relative to the other fibers.

It is interesting to see the degradation rate of the Celion 6000/PMR-15 composites in air over an extended temperature range. An Arrhenius plot for the air-aged composites at 260, 288, 343, 371, and 343 °C is presented in figure 11. The activation energy values calculated from these data are also presented in the figure. The activation energy for the air-aged material, at temperatures above 316 °C, varies with changing temperature; therefore, the Arrhenius relationship is not valid over the temperature range studied here. The calculated energy increases with increasing temperature, more than doubling over the temperature range investigated. Since predictions based on the Arrhenius equation are not valid over the temperature range studied here, figure 11 points out the necessity of conducting isothermal air-aging tests at more than one temperature over the expected range of use temperatures. Also, because of the data presented in this figure, the validity of calculated oxidation activation energies for any polymer matrix composites is suspect.

#### General Behavior

The thermo-oxidative stability rating of the bare fibers that were studied are: (1) ceramic, (2) T-40R, and (3) Celion 6000. It is evident from figure 2 that the thermo-oxidative stability of the composites, with these fibers as reinforcement, do not rank the same as the bare fibers. It is also apparent in figure 2 that the four ceramic fiber-reinforced composites lose weight at a rate equal to or slightly faster than the calculated rule-of-mixtures value. The presence of these fibers apparently has little effect on the matrix degradation process.

When the mechanical properties listed in table III are compared with the weight loss data in figure 2, there is no correlation between mechanical properties and thermo-oxidative stability. The Celion 6000/PMR-15 composite was the most thermally stable of the four types of composites studied. This material displayed high flexural strength and good interlaminar shear strength. The magnitudes of these property values indicated that there was a good interfacial bond between the fiber surface and the matrix material. In contrast, the unsized and PVA sized Nicalon fiber-reinforced PMR-15 composites exhibited flexural strengths of about 60 percent of that possessed by the Celion 6000 fiber-reinforced composites and about one-third of the interlaminar shear strength.

These materials possessed thermo-oxidative stabilities that were inferior to those of the Celion 6000 reinforced composites. In contrast, the BMIC Nicalon fiber-reinforced composites possessed better mechanical properties than did the Celion 6000 fiber-reinforced composites; however, the thermo-oxidative stability, as determined from this study, was inferior to that of the Celion 6000, T-40, and Nextel reinforced composites. This may have been due to a possible degradation of the sizing during cure. The PMR-15 cure temperature was well above that of a BMIC composite. The T-40 unsized graphite fiber-reinforced composites possessed mechanical properties of about the same magnitude as did the ceramic fibers but had a thermal stability equal to or better than the ceramic composites.

#### SUMMARY OF RESULTS

For the isothermal study that was conducted and reported herein, the results can be summarized as follows:

1. The thermo-oxidative stability of the T-40 bare, unsized graphite fiber in air is significantly greater than that of bare, unsized Celion 6000 fiber.
2. The increase in Celion 6000 fiber surface area with aging time and weight loss is significantly greater than that of the T-40R fiber.
3. The T-40R fiber-reinforced composites possess lower flexural and ILSS properties than those composites fabricated with Celion 6000 reinforcement.
4. Only the BMIC sized Nicalon ceramic fiber-reinforced composite possessed flexural and ILSS properties that are superior to those of the graphite fiber composites. The others have inferior properties.
5. Ceramic fiber-reinforced composites that are subjected to thermo-oxidative degradation in air do not display size effects on the weight loss rate. Specimens of different sizes lose weight at the same rate.
6. Composites reinforced with T-40R fibers do exhibit a kind of size effect on the thermo-oxidation rate in air, but not in the way observed with Celion 6000/PMR-15 composites.

The three conclusions that can be drawn from this work are:

1. Bare fiber thermo-oxidative stability is not always reflected in composite stability.

2. Composite mechanical properties ranking is not always reflected in ranking according to thermo-oxidative stability.

3. In order to obtain a true indication of the thermo-oxidative stability of a composite material, isothermal aging tests must be run at more than one temperature over the expected use range.

#### REFERENCES

1. Hanson, M.P.; and Serafini, T.T.: Effects of Thermal and Environmental Exposure on the Mechanical Properties of Graphite/Polyimide Composites. Space Shuttle Materials, SAMPE, 1971, pp. 31-38.
2. Gibbs, H.H.; Wendt, R.C.; and Wilson, F.C.: Carbon Fiber Structure and Stability Studies. Proceedings of the 33rd Annual Conference, Reinforced Plastics/Composites Institute, The Society of Plastics Industry, 1978, pp. 24F1-24F9.
3. Eckstein, B.H.: Oxidation of Carbon Fibres in Air Between 230° and 375 °C. Fibre Sci. Technol., vol. 14, no. 2, Oct. 1981, pp. 139-156.
4. Scola, D.A.: Thermo-Oxidative Stability of Graphite Fiber/PMR-15 Polyimide Composites at 350 °C. High Temperature Polymer Matrix Composites, NASA CP-2385, 1985, pp. 217-242.
5. Bowles, K.J.; and Meyers, A.E.: Specimen Geometry Effects on Graphite/PMR-15 Composites During Thermo-Oxidative Aging. Materials Sciences for the Future, J.L. Bauer and K. Dunaetz, eds., SAMPE, 1986, pp. 1285-1299.
6. Bowles, K.J.; and Nowak, G.: Thermo-Oxidative Stability Studies of Celion 6000/PMR-15 Unidirectional Composites, PMR-15, and Celion 6000 Fiber. J. Compos. Mater., vol. 22, no. 10, Oct. 1988, pp. 966-985.
7. Vannucci, R.D.: PMR-15 Polyimide Modifications for Improved Prepreg Tack. Proceedings of the 1982 National Technical Conference: The Plastic's ABC's, Society of Plastics Engineers, 1982, pp. 131-133. (NASA TM-82951).
8. Vannucci, R.D.: PMR Polyimide Compositions for Improved Performance at 371 °C. Advanced Materials Technology '87, R. Carson, et al., eds., SAMPE, 1987, pp. 602-612.
9. Materne, H.P., Jr.; and Kuhbander, R.J.: Silicon Carbide Filament-Reinforced Epoxy Resin Composites. Advanced Fibrous Reinforced Composites, SAMPE, 1966, pp. A-31 to A-39.

TABLE I. - FIBER PROPERTIES

Material	Property				
	Tensile strength, MPa (ksi)	Tensile modulus, GPa (msi)	Strain at failure, percent	Density, g/cm <sup>3</sup>	Fiber diameter, mm
Celion 6000 fiber	3890 (550)	235.2 (34)	1.65	1.77	7.1
Nicalon fiber	2700 (400)	200 (29)	1.38	2.55	10-15
T-40R graphite fiber	3640 (528)	296.5 (43)	1.23	1.775	10
Nextel 312 fiber	1380-1724 (200-250)	151.7 (22)	0.91-1.14	2.7	10-12

TABLE II. - ACTIVATION ENERGIES FROM ARRHENIUS PLOTS FOR DIFFERENT COMPOSITES, REINFORCEMENTS, AND PMR-15

[Log rate = log A - E<sub>A</sub>/2.303 x RT, Kcal/g-mol.]

Material	Activation energy, E <sub>A</sub> , Kcal/g-mol
Celion 6000/PMR-15, 288-316 °C	28.6
Celion 6000/PMR-15, 316 °C	45.8
PVA sized Nicalon/PMR-15	61.6
Stripped Nicalon/PMR-15	67.9
Sized Nextel/PMR-15	79.5
Unsize T-40R/PMR-15	43.6
Celion 6000 fiber	38.6 to -41.3
T-40R fiber	30.4
PMR-15 resin	30.6

TABLE III. - MECHANICAL PROPERTIES OF PMR-15 MATRIX COMPOSITES WITH DIFFERENT FIBERS AT ROOM TEMPERATURE

Material	Property				
	Flexural strength, GPa (ksi)	Flexural strength (rule of mixtures), GPa (ksi)	Flexural modulus, GPa (msi)	Interlaminar shear strength, MPa (ksi)	Fiber, vol %
Celion 6000 (U) <sup>a</sup>	1.65 (240.0)	2.28 (330.0)	113.9 (16.3)	103.4 (15.0)	60.0
T-40R (U) <sup>a</sup>	0.88 (128.0)	2.03 (294.0)	75.0 (10.9)	75.0 (10.9)	55.7
Nicalon (S) <sup>b</sup>	1.0 (147.3)	1.45 (210.4)	88.0 (12.8)	35.6 (5.2)	52.6
Nicalon (PVA) <sup>c</sup>	0.9 (129.0)	1.35 (196.0)	61.0 (8.8)	35.6 (5.2)	49.0
Niaclon (BMIC) <sup>d</sup>	2.05 (296.8)	1.50 (220.0)	105.0 (15.0)	118.4 (16.2)	55.0
Nextel (U) <sup>a</sup>	0.5 (72.5)	0.68 (98.4)	28.5 (4.1)	45.8 (6.6)	49.2

<sup>a</sup>U = unsized.

<sup>b</sup>S = stripped.

<sup>c</sup>PVA = polyvinyl acetate sizing.

<sup>d</sup>BMIC = bismaleimid sizing.

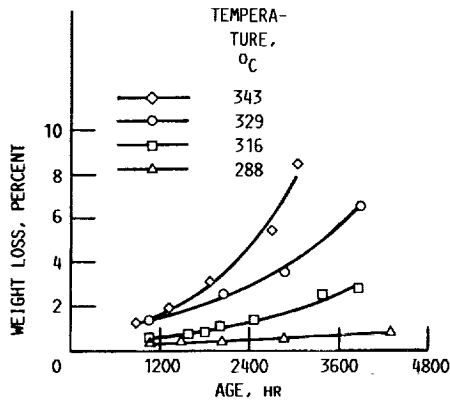


FIGURE 1. - AIR-AGING OF BARE, UNSIZED T-40R FIBER.

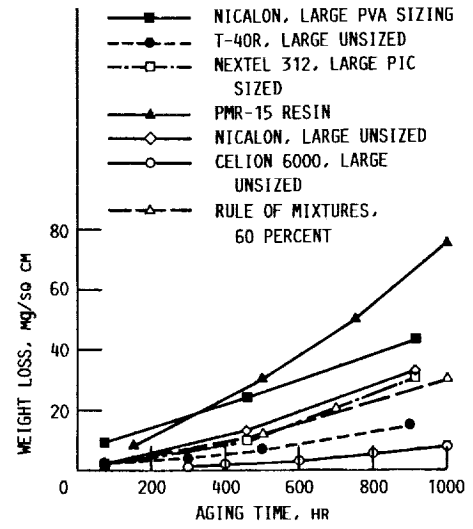


FIGURE 2. - WEIGHT LOSS OF PMR-15 COMPOSITES AGED IN AIR AT 316 °C.

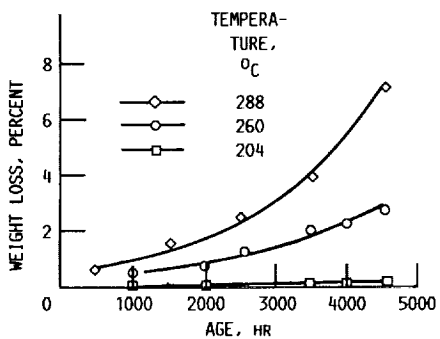


FIGURE 3. - AIR-AGING OF CELION 6000/PMR-15 UNIDIRECTIONAL COMPOSITES.

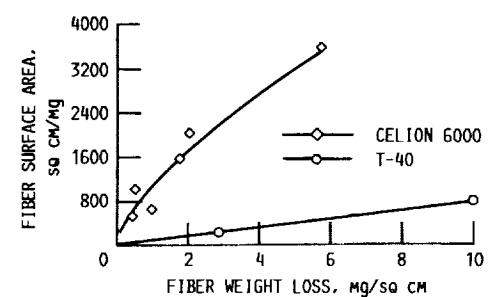


FIGURE 4. - FIBER SURFACE AREA AS FUNCTION OF WEIGHT LOSS. GRAPHITE FIBERS.

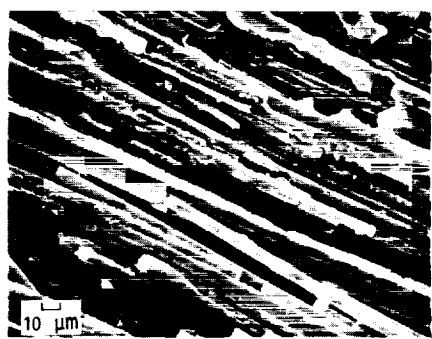


FIGURE 5. - CELION 6000/PMR-15 FRACTURE SURFACE.



FIGURE 6. - UNSIZED NICALON/PMR-15 FRACTURE SURFACE. DARK AREA IS THE FIBER.

ORIGINAL PAGE IS OF POOR QUALITY

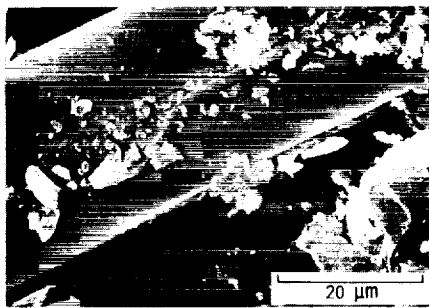


FIGURE 7. - BMIC SIZED NICALON REINFORCED COMPOSITE CLEAVED SURFACE.

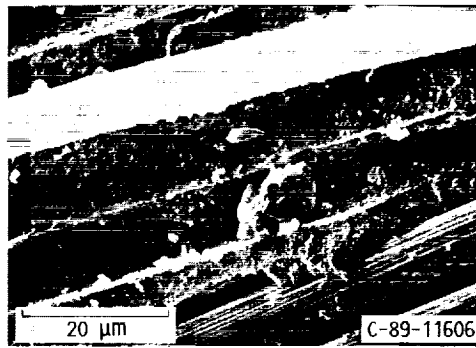
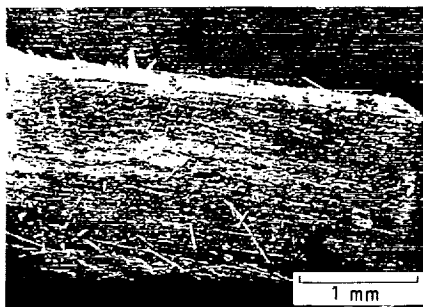
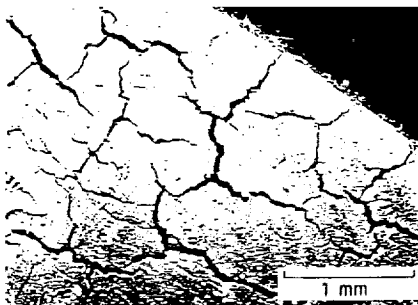


FIGURE 8. - CLEAVED SURFACE OF T-40R UNIDIRECTIONAL COMPOSITE SHOWING INTERFACIAL FAILURE.



(a) T-40R/PMR-15 COMPOSITE AFTER 889 HR OF AGING.



(b) CELION 6000/PMR-15 COMPOSITE AFTER 1212 HR OF AGING. CRACKS RUN PARALLEL TO FIBERS.

FIGURE 9. - END VIEWS OF PMR-15 COMPOSITE AFTER AGING IN AIR AT 316 °C.

ORIGINAL PAGE IS OF POOR QUALITY

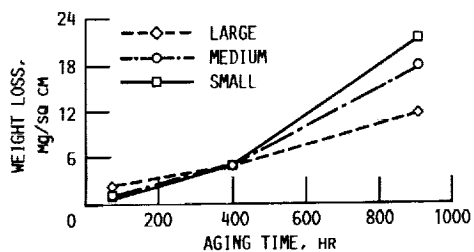


FIGURE 10. - WEIGHT LOSS OF T-40R FIBER-REINFORCED COMPOSITES AGED IN AIR AT 316 °C.

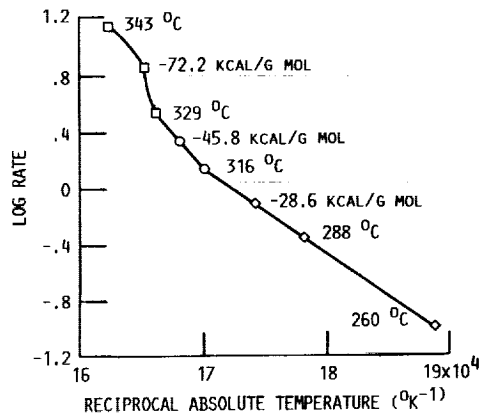


FIGURE 11. - ARRHENIUS PLOTS FOR CELION 6000/PMR-15 UNIDIRECTIONAL COMPOSITES.

1. Report No. NASA TM-102439		2. Government Accession No.		3. Recipient's Catalog No.	
4. Title and Subtitle Thermo-Oxidative Stability Studies of PMR-15 Polymer Matrix Composites Reinforced With Various Continuous Fibers				5. Report Date	
				6. Performing Organization Code	
7. Author(s) Kenneth J. Bowles				8. Performing Organization Report No. E-5208	
				10. Work Unit No. 510-01-0A	
9. Performing Organization Name and Address National Aeronautics and Space Administration Lewis Research Center Cleveland, Ohio 44135-3191				11. Contract or Grant No.	
				13. Type of Report and Period Covered Technical Memorandum	
12. Sponsoring Agency Name and Address National Aeronautics and Space Administration Washington, D.C. 20546-0001				14. Sponsoring Agency Code	
15. Supplementary Notes Prepared for the 35th International SAMPE Symposium and Exhibition, Anaheim, California, April 2-5, 1990.					
16. Abstract An experimental study was conducted to measure the thermo-oxidative stability of PMR-15 polymer matrix composites reinforced with various fibers and to observe differences in the way they degrade in air. The fibers that were studied included graphite and the thermally stable Nicalon and Nextel ceramic fibers. Weight loss rates for the different composites were assessed as a function of mechanical properties, specimen geometry, fiber sizing, and interfacial bond strength. Differences were observed in rates of weight loss, matrix cracking, geometry dependency, and fiber-sizing effects. It was shown that Celion 6000 fiber-reinforced composites do not exhibit a straight-line Arrhenius relationship at temperatures above 316 °C.					
17. Key Words (Suggested by Author(s)) Composites; Polyimide; Graphite fiber; Ceramic fiber; Oxidation; Interfaces; Aging			18. Distribution Statement Unclassified—Unlimited Subject Category 24		
19. Security Classif. (of this report) Unclassified		20. Security Classif. (of this page) Unclassified		21. No. of pages 14	22. Price* A03

